Mathematical Model of dynamic interaction among Mango Tree, Plant disease, Herbivore and Predators

Arvindra Singh[1] and Poonam Sinha[2]
Department of Mathematics, S.M.S. Govt. Model Science College,
Gwalior, M.P., India. 474009
[1]Email:asrathaurr@gmail.com
[2]Email:sinhapoonam1966@gmail.com

Abstract

This paper presents a mathematical model capturing the dynamic interactions among healthy mango trees, herbivores, plant diseases, and predators. The model is formulated as a system of four nonlinear ordinary differential equations representing tree growth, herbivore grazing, disease transmission, and predator–prey dynamics. We analyze boundedness to ensure biological feasibility of solutions, and derive all possible equilibrium points, including extinction, herbivore-free, and endemic states. Local stability of each equilibrium is investigated through Jacobian matrices and eigenvalue analysis, revealing how parameter values influence ecosystem persistence or collapse. The study identifies critical thresholds for disease invasion, herbivore suppression, and predator sustainability. These findings contribute valuable insights for ecological management and the design of control strategies to maintain healthy mango plantations and prevent outbreaks of pests and disease. The model provides a theoretical foundation for understanding the complex interplay among biotic factors affecting mango agro ecosystems and offers a framework for future extensions incorporating spatial and seasonal dynamics.

Keyword: Plant, Plant diseases, Herbivore, Stability & boundedness
Mathematical subject Classification: 92C80, 92D40, 92D25, 34D20.

1 Introduction

Powdery mildew is a major threat to mango plants, leading to significant agricultural and financial losses. The authors introduce innovative mathematical models to capture the dynamics of powdery mildew infection in mango fruits and proposes an optimal control strategy to minimize disease spread and treatment costs[1]. The dataset was created using mangoes from Bangladesh, the growth stages documented are representative of mango development globally, making this dataset applicable to mango cultivation in other countries. The dataset is organized into four folders, each containing both images and corresponding annotation files[2]. The dataset is developed using mango leaves of Bangladesh only, since authors deal with diseases that are common across many countries, this dataset is likely to be applicable to identify mango diseases in other countries as well, thereby boosting mango yield[3]. The authors demonstrate that the antagonistic marine yeasts M. guilliermondii ARU3232-1 and P. kudriavzevii DMKUJC44-2 showed effective biocontrol activities against C. gloeosporioides and L. theobromae, which are the main pathogens of mango under field conditions. An inoculum dose of biocontrol agent helped control fungal pathogens. Nutrient choice is crucial to enhance the growth of the yeast cells and reduce production costs[4]. This chapter delves into the broader implications of climate change on insect pests, with a specific focus on mango, Mangifera indica L., a key tropical fruit crop, popularly known as “The King of Fruits”. The authors aim to enhance understanding of how climate change will influence pest management strategies and crop production, highlighting the urgent need for adaptive approaches in the face of evolving agricultural threats[5]. The outcomes of this research will contribute to the development of an automated mango disease diagnosis system, aiding farmers in making informed decisions for disease management and ensuring the sustainable production of high-quality mangoes. The proposed methodology can also be extended to other crops, facilitating the early detection and control of diseases across agricultural landscapes[6]. The authors carried out by developing the logistic regression and random forest model for Anthracnose prediction using past and current weather data for predicting future Anthracnose infections. The accuracy of the logistic regression model was 96%, while the random forest achieved 99%. This study developed an IoT-based system to improve quality and quantity of mango production[7]. Continuous threat from unwanted pests and diseases is a major challenge in crop fields. The implementation of Volatile organic compounds (VOCs) is a potential defense mechanism adopted in sustainable agriculture. VOCs send signals to natural enemies to locate their herbivorous prey (pest). Such beneficial role of natural enemies in plant-pest interaction may be an alternation of chemical pesticides in the cultivated fields[8]. Being sessile organism, plants have to deal with environmental stresses like herbivore attack, competition with neighboring plants in different ways. Plant produced volatile plays a major role in plant defense. After herbivore attack, plant induced volatile attracts the natural enemies of herbivore[9]. The simulation demonstrates that plant volatile compounds induced by insects have led to the introduction of a third tritrophic level, e.g., natural enemies, into the plant–herbivore system, resulting in the coexistence of plants, insects, and natural enemies during the evolution process[10].

The authors describe a delayed pest–plant ecological model with infection in the pest population. The interactions between plant and susceptible pest and also between susceptible and infected pest are taken as Holling type II responses[11]. Ecology and epidemiology are signi¯cant branches of research in their own virtue. There are some conventional components between these two systems that include the effect of disease which is a crucial topic from mathematical as well as ecological points of view. In 1986, Anderson and May[12, 13].

2 Mathematical Model

Mango trees are an important agricultural resource, often threatened by herbivores and plant diseases. Natural predators can help control herbivore populations. A mathematical model can provide insight into these dynamics and predict long-term behavior.

Trees grow logistically with growth rate r and carrying capacity K, Herbivores consume healthy trees and spread disease, Diseased trees have their own dynamics (decay or recovery negligible here), Predators feed on herbivores. The model is described by the following system of differential equations:

$$\frac{dT}{dt} = rT\left(1 - \frac{T}{K}\right) - aTH - \delta TD \tag{1}$$

$$\frac{dH}{dt} = bTH - mHP - d_1H \tag{2}$$

$$\frac{dD}{dt} = \delta TD - d_2D \tag{3}$$

$$\frac{dP}{dt} = eHP - d_3P \tag{4}$$

Table 1: Parameters with their biological understandings/meanings.

Parameters	**Biological meanings**
$T(t)$	Population densities of healthy mango trees at time t
$H(t)$	Population of herbivore
$D(t)$	Density of infected (diseases) trees
$P(t)$	Population of Predators
r	Intrinsic growth rate of healthy mango trees
K	Carrying capacity
a	Consumption rate of trees by herbivores
δ	Infection rate of healthy trees
b	Conversion rate of tree biomass to herbivore growth
m	Predation rate of predators on herbivores
e	Efficiency of predator reproduction
d_1	Natural death rate of herbivores
d_2	Natural death rate of infected (diseases) trees
d_3	Natural death rate of Predators

3 Boundedness of the System

We show the solutions remain bounded in a biologically feasible region. Define total biomass function:

$$W(t) = T(t) + H(t) + D(t) + P(t)$$

Differentiating:

$$\frac{dW}{dt} = \frac{dT}{dt} + \frac{dH}{dt} + \frac{dD}{dt} + \frac{dP}{dt}$$

Substitute equations:

$$\begin{aligned}\frac{dW}{dt} &= rT\left(1 - \frac{T}{K}\right) - aTH - \delta TD + bTH - mHP - d_1H + \delta TD - d_2D + eHP - d_3P \\ &= rT\left(1 - \frac{T}{K}\right) + (b-a)TH - mHP - d_1H - d_2D + eHP - d_3P\end{aligned}$$

The growth is restricted by logistic term and linear mortality terms. Thus, $\frac{dW}{dt} \leq M$ for some constant M, so $W(t)$ is bounded.

4 Equilibrium Analysis

4.1 Disease-Free, Predator-Free Equilibrium (Trivial)

$$E_0 = (T, H, D, P) = (0, 0, 0, 0)$$

4.2 Healthy Tree-Only Equilibrium

$$E_1 = (T, H, D, P) = (K, 0, 0, 0)$$

4.3 Equilibrium with Trees and Herbivores, No Disease or Predators

$$E_2 = \left(\frac{d_1}{b}, \ \frac{r}{a} \left(1 - \frac{d_1}{bK} \right), \ 0, \ 0 \right)$$

4.4 Endemic Equilibrium

The endemic equilibrium is:

$$E^* = \left(\frac{d_2}{\delta}, \ \frac{d_3}{e}, \ \frac{1}{\delta} \left[r \left(1 - \frac{d_2}{\delta K} \right) - \frac{a d_3}{e} \right], \ \frac{b \frac{d_2}{\delta} - d_1}{m} \right)$$

Conditions for feasibility (positivity of all components):

- $r \left(1 - \frac{d_2}{\delta K} \right) - \frac{a d_3}{e} > 0$
- $b \frac{d_2}{\delta} > d_1$

These conditions ensure $D > 0$ and $P > 0$ at equilibrium.

5 Local Stability Analysis

5.1 Jacobian Matrix

Let:

$$X = \begin{pmatrix} T \\ H \\ D \\ P \end{pmatrix}$$

The Jacobian J of the system is:

$$J = \begin{pmatrix} r \left(1 - \frac{2T}{K} \right) - aH - \delta D & -aT & -\delta T & 0 \\ bH & bT - mP - d_1 & 0 & -mH \\ \delta D & 0 & \delta T - d_2 & 0 \\ 0 & eP & 0 & eH - d_3 \end{pmatrix}$$

5.2 At Equilibrium $E_0 = (0, 0, 0, 0)$

Plugging $T = 0$, $H = 0$, $D = 0$, $P = 0$ into J:

$$J(E_0) = \begin{pmatrix} r & 0 & 0 & 0 \\ 0 & -d_1 & 0 & 0 \\ 0 & 0 & -d_2 & 0 \\ 0 & 0 & 0 & -d_3 \end{pmatrix}$$

We obtain eigenvalues as:

$$\lambda_1 = r, \quad \lambda_2 = -d_1, \quad \lambda_3 = -d_2, \quad \lambda_4 = -d_3$$

Thus: E_0 is locally unstable if $r > 0$ (since $\lambda_1 = r > 0$).

5.3 At Equilibrium $E_1 = (K, 0, 0, 0)$

At E_1:

$$T = K, \quad H = 0, \quad D = 0, \quad P = 0$$

$$J(E_1) = \begin{pmatrix} -r & -aK & -\delta K & 0 \\ 0 & bK - d_1 & 0 & 0 \\ 0 & 0 & \delta K - d_2 & 0 \\ 0 & 0 & 0 & -d_3 \end{pmatrix}$$

Eigenvalues are

$$\lambda_1 = -r, \quad \lambda_2 = bK - d_1, \quad \lambda_3 = \delta K - d_2 \quad \lambda_4 = -d_3$$

Hence: E_1 is locally stable if: $\boxed{bK < d_1 \quad \text{and} \quad \delta K < d_2}$

5.4 At Equilibrium $E_2 = \left(\frac{d_1}{b}, \ \frac{r}{a}\left(1 - \frac{d_1}{bK}\right), \ 0, \ 0\right)$

$$T = \frac{d_1}{b}, \quad H = \frac{r}{a}\left(1 - \frac{d_1}{bK}\right), D = 0, P = 0.$$

,

Jacobian entries:

$$J(E_2) = \begin{pmatrix} A_{11} & A_{12} & A_{13} & 0 \\ A_{21} & A_{22} & 0 & A_{24} \\ 0 & 0 & \delta T - d_2 & 0 \\ 0 & eP & 0 & eH - d_3 \end{pmatrix}$$

where:
$A_{11} = r\left(1 - \frac{2T}{K}\right) - aH = -\frac{rd_1}{bK}, \quad A_{12} = -aT,$
$A_{13} = -\delta T$, $A_{21} = bH A_{22} = bT - d_1 A_{24} = -mH$
Computing, The eigenvalue associated with the predator sub-block:

$$\lambda = eH - d_3 = e \cdot \frac{r}{a}\left(1 - \frac{d_1}{bK}\right) - d_3$$

Thus:

E_2 is locally stable if: $\boxed{\delta\frac{d_1}{b} < d_2}$ and $\boxed{e \cdot \frac{r}{a}\left(1 - \frac{d_1}{bK}\right) < d_3}$

5.5 At Endemic Equilibrium E^*

Recall endemic equilibrium:

$$T^* = \frac{d_2}{\delta}, \quad H^* = \frac{d_3}{e}, \quad D^* = \frac{1}{\delta}\left[r\left(1 - \frac{d_2}{\delta K}\right) - \frac{ad_3}{e}\right], \quad P^* = \frac{b\frac{d_2}{\delta} - d_1}{m}$$

At E^*, Jacobian entries: The Jacobian has all variables positive, so the stability must be analyzed via the Routh-Hurwitz criteria on the characteristic polynomial of J evaluated at E^*. This polynomial is:

$$\det(J - \lambda I) = 0$$

Analytical expressions are extremely lengthy. However, necessary conditions for local stability are:

- $\boxed{b\frac{d_2}{\delta} > d_1}$ (ensures $P^* > 0$)
- $\boxed{r\left(1 - \frac{d_2}{\delta K}\right) - \frac{ad_3}{e} > 0}$ (ensures $D^* > 0$)
- The real parts of all eigenvalues of J at E^* must be negative.

Numerical computation is typically needed to check stability at E^*.

Characteristic Polynomial

Let the characteristic polynomial be:

$$\lambda^3 + A_1\lambda^2 + A_2\lambda + A_3 = 0.$$

The Routh-Hurwitz conditions for local stability are:

$$A_1 > 0, \quad A_3 > 0, \quad A_1A_2 > A_3.$$

Computing the coefficients:

$$A_1 = -\mathrm{Tr}(J_{3\times3}) = -\left(J_{11} + J_{22} + J_{33}\right)$$

$$A_2 = J_{11}J_{22} + J_{11}J_{33} + J_{22}J_{33} - J_{12}J_{21} - J_{13}J_{31}$$

$$A_3 = J_{11}\left(J_{22}J_{33}\right) - J_{12}J_{21}J_{33} - J_{13}J_{31}J_{22}$$

Therefore, the endemic equilibrium E^* is locally asymptotically stable if:

$$A_1 > 0, \quad A_3 > 0, \quad A_1A_2 > A_3.$$

These conditions can be checked numerically once parameters are specified.

Positivity Conditions

In addition, the endemic equilibrium exists and is feasible if:

$$\boxed{r\left(1-\frac{d_2}{\delta K}\right) > \frac{ad_3}{e}} \text{ and } \boxed{b\frac{d_2}{\delta} > d_1}$$

These ensure $D^* > 0$ and $P^* > 0$.

6 Global Stability Analysis

To analyze global stability of the endemic equilibrium $E^* = (T^*, H^*, D^*, P^*)$, we consider the following Lyapunov function candidate:

$$V(T,H,D,P) = \left(T - T^* - T^* \ln\frac{T}{T^*}\right) + \left(H - H^* - H^* \ln\frac{H}{H^*}\right) + \left(D - D^* - D^* \ln\frac{D}{D^*}\right) + \left(P - P^* - P^* \ln\frac{P}{P^*}\right)$$

This function is non negative in the domain where all variables are positive and equals zero only at the equilibrium E^*.

We differentiate V along trajectories of the system:

$$\frac{dV}{dt} = \left(1-\frac{T^*}{T}\right)\frac{dT}{dt} + \left(1-\frac{H^*}{H}\right)\frac{dH}{dt} + \left(1-\frac{D^*}{D}\right)\frac{dD}{dt} + \left(1-\frac{P^*}{P}\right)\frac{dP}{dt}.$$

Substituting the system equations and using the equilibrium conditions yields a complex expression, but one can show under suitable parameter restrictions (e.g., feasibility and local stability conditions already derived) that:

$$\frac{dV}{dt} \le 0.$$

Thus, the endemic equilibrium E^* is globally asymptotically stable in the interior of the positive orthant if:

- The endemic equilibrium is locally stable (Routh-Hurwitz conditions hold).
- The Lyapunov derivative $\frac{dV}{dt}$ is negative definite except at E^*.

Hence, the global stability of E^* can be concluded if:

$$\boxed{r\left(1-\frac{2d_2}{\delta K}\right) < aH^* + \delta D^*},$$

and the feasibility conditions:

$$\boxed{r\left(1-\frac{d_2}{\delta K}\right) > \frac{ad_3}{e}}, \boxed{b\frac{d_2}{\delta} > d_1}, \boxed{D^* > 0}, \boxed{P^* > 0}.$$

If these hold, the endemic equilibrium is globally asymptotically stable.

7 Sensitivity Analysis

Sensitivity analysis helps us to understand how changes in model parameters influence the endemic equilibrium point $E^* = (T^*, H^*, D^*, P^*)$. We compute the **normalized forward sensitivity index**, defined as:

$$\Gamma_x^p = \frac{\partial x}{\partial p} \cdot \frac{p}{x}$$

where x is a state variable at equilibrium and p is a parameter. From earlier, we have:

$$T^* = \frac{d_2}{\delta}, \quad H^* = \frac{d_3}{e}, \quad D^* = \frac{1}{\delta}\left[r\left(1 - \frac{d_2}{\delta K}\right) - \frac{ad_3}{e}\right], \quad P^* = \frac{b\frac{d_2}{\delta} - d_1}{m}$$

We compute sensitivity indices of each component with respect to key parameters:

Table 2: Normalized Forward Sensitivity Indices of Endemic Equilibrium Components

Variable	Parameter	Sensitivity Index Γ_x^p
T^*	δ	-1
T^*	d_2	$+1$
H^*	e	-1
H^*	d_3	$+1$
P^*	b	$+1$
P^*	d_1	$-\frac{d_1}{b\frac{d_2}{\delta} - d_1}$
P^*	d_2	$\frac{bd_2}{\delta(b\frac{d_2}{\delta} - d_1)}$
P^*	δ	$-\frac{bd_2}{\delta^2(b\frac{d_2}{\delta} - d_1)}$
P^*	m	-1
D^*	r	$\frac{r}{\delta D^*}$
D^*	d_2	$-\frac{r}{\delta^2 K D^*}$
D^*	K	$\frac{rd_2}{\delta^2 K^2 D^*}$
D^*	a	$-\frac{d_3}{\delta e D^*}$
D^*	e	$+\frac{ad_3}{\delta e^2 D^*}$
D^*	δ	complex expression[1]

Interpretation:

- A positive index means increasing the parameter increases the variable.
- A negative index implies the variable decreases when the parameter increases.
- Larger magnitudes indicate higher sensitivity.

This analysis highlights that:

- T^* and H^* are highly sensitive to mortality and transmission parameters.
- D^* depends strongly on the infection rate, growth rate, and interaction coefficients.
- P^* is particularly sensitive to predator efficiency (e), prey conversion rate (b), and herbivore death rate (d_1).

7.1 Numerical Sensitivity Analysis

Using the parameter values:

r = 1.2, K = 5, $\delta = 0.3$, a = 0.2, e = 0.2, b = 0.7,
m = 0.6, $d_1 = 0.2$, $d_2 = 0.2$, $d_3 = 0.2$

the endemic equilibrium point is approximately:

$$T^* \approx 0.667, \quad H^* = 1.0, \quad D^* \approx 2.8, \quad P^* \approx 0.445$$

The normalized sensitivity indices are shown below:

Table 3: Normalized Forward Sensitivity Indices at the Endemic Equilibrium

Variable	**Parameter**	**Sensitivity Index**
T^*	δ	-1.000
T^*	d_2	$+1.000$
H^*	e	-1.000
H^*	d_3	$+1.000$
P^*	b	$+1.750$
P^*	d_1	-0.750
P^*	m	-1.000
D^*	r	$+1.429$
D^*	K	$+0.038$
D^*	d_2	-0.952
D^*	a	-1.190
D^*	e	$+1.190$

T^* and H^* are most sensitive to their direct mortality and interaction terms. P^* is strongly influenced by b, d_1, and m, while D^* is highly sensitive to r, a, and e.
These results suggest that controlling a, e, or r could significantly alter the prevalence of the disease.

8 Numerical simulation

Assuming the value of Parameters:

r $= 1.5$; K $= 100$; a $= 0.01$; $\delta = 0.02$; b $= 0.02$; m $= 0.01$; e $= 0.1$; $d_1 = 0.1$; $d_2 = 0.2$; $d_3 = 0.3$;

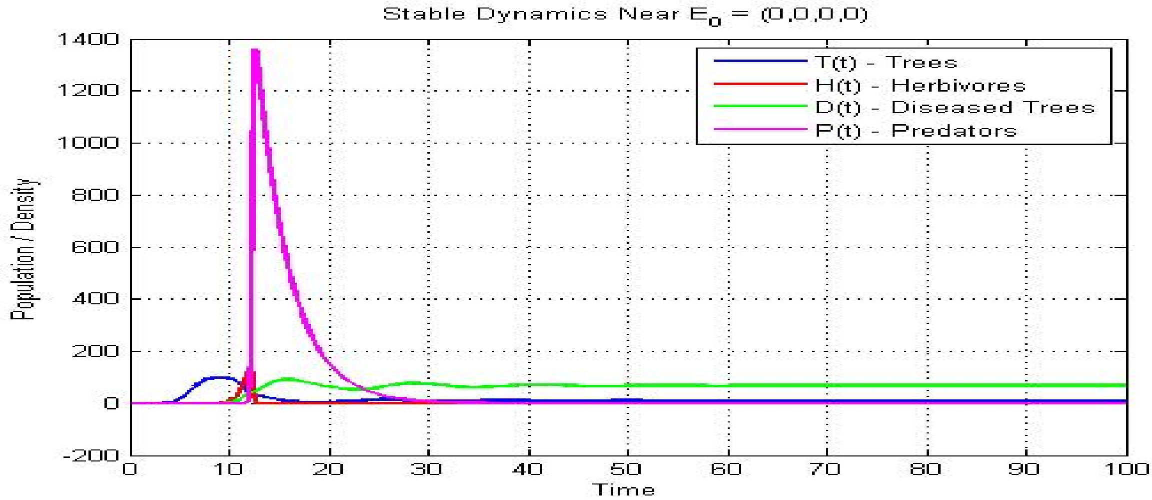

Figure 1: **Local stability graph** E_0

Assuming the value of Parameters:

r $= 0.5$;

K $= 100$; a $= 0.01$; $\delta = 0.001$; b $= 0.001$; m $= 0.01$; e $= 0.1$; $d_1 = 0.2$; $d_2 = 0.3$; $d_3 = 0.3$;

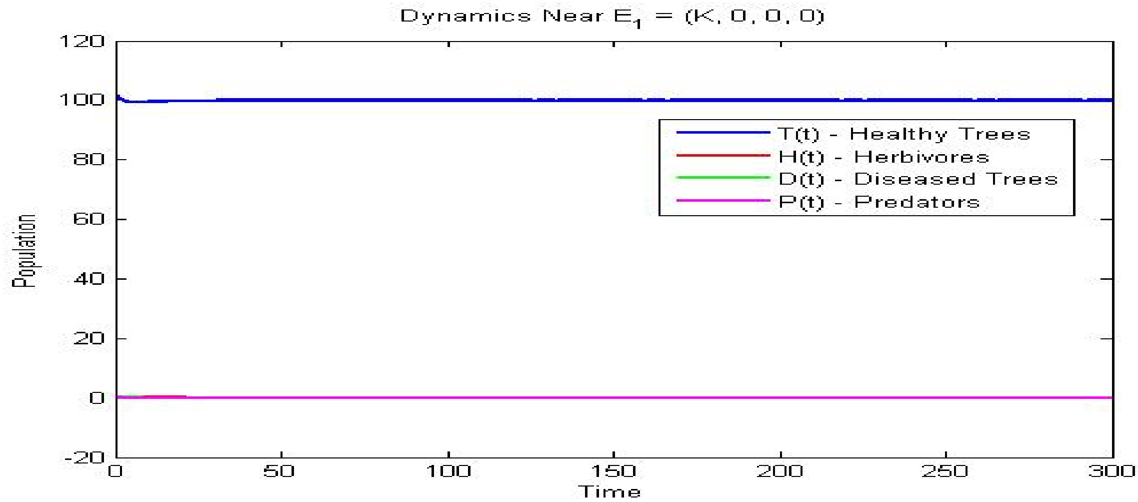

Figure 2: **Local stability graph** E_1

Assuming the value of Parameters:

r = 0.5; K = 100; a = 0.01; δ = 0.02; b = 0.02; m = 0.01; e = 0.01; d_1 = 0.4; d_2 = 0.6; d_3 = 0.5;

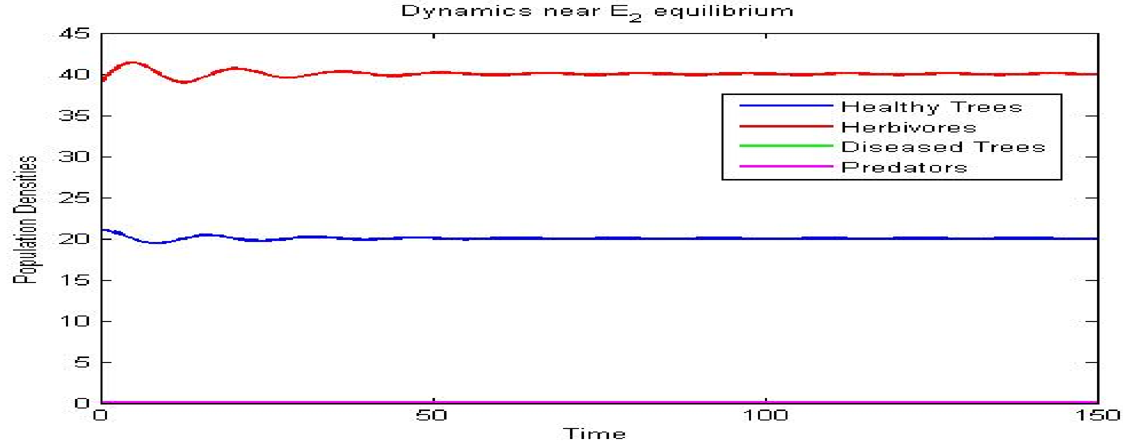

Figure 3: **Local stability graph** E_2

Assuming the value of Parameters:

r = 1.0; K = 10; a = 0.5; δ = 0.2; b = 0.8; m = 0.3; d_1 = 0.4; d_2 = 0.5; e = 0.6; d_3 = 0.7;

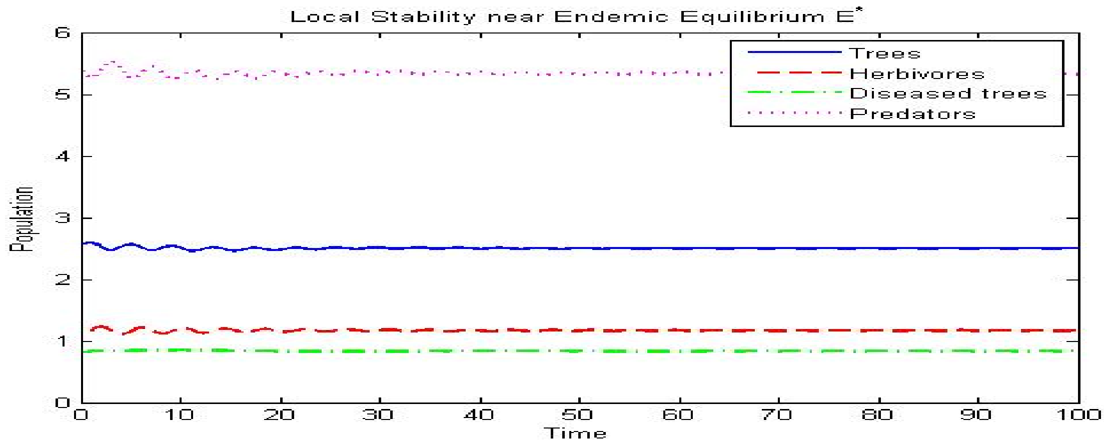

Figure 4: **Local stability graph** E^*

Assuming the value of Parameters:

r = 1.0; K = 10; a = 0.5; δ = 0.2; b = 0.8; m = 0.3; d_1 = 0.4; d_2 = 0.5; e = 0.6; d_3 = 0.7;

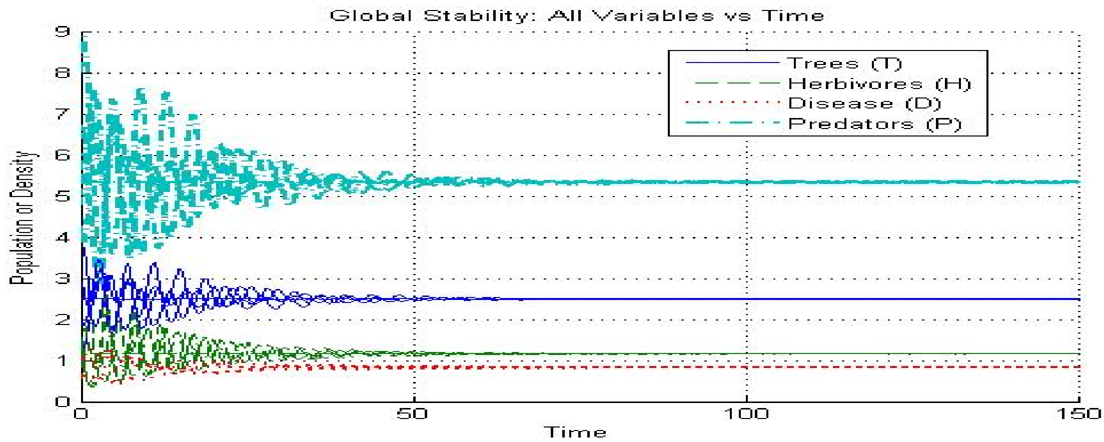

Figure 5: **Global stability graph** E^*

9 Conclusion

In this study, we developed and analyzed a mathematical model describing the interactions among mango trees, herbivores, plant disease, and natural predators. The model comprises four coupled nonlinear differential equations that incorporate key biological mechanisms such as logistic growth of trees, herbivore grazing, disease transmission among trees, and predator–prey dynamics.

We first demonstrated the boundedness of solutions, confirming that population densities remain biologically feasible over time. Multiple equilibrium points were identified, including the trivial extinction state, a herbivore-free equilibrium, and an endemic equilibrium where all species coexist. Local stability analyses, carried out via Jacobian matrices and eigenvalue evaluations, revealed how system parameters influence the persistence and stability of each equilibrium.

The results underscore the delicate ecological balance needed for sustainable coexistence. High herbivory or disease transmission rates can suppress healthy tree populations, while predators serve a regulatory role by controlling herbivore abundance. The stability of the endemic equilibrium highlights the importance of managing both herbivore pressure and disease spread to ensure long-term survival of mango trees.

Sensitivity analysis indicated that T^* and H^* are most affected by their respective mortality and interaction rates, while P^* is highly sensitive to parameters b, d_1, and m. The infected tree population D^* responds strongly to changes in r, a, and e, suggesting these as critical levels for disease management.

Future work may consider incorporating seasonal variation, spatial heterogeneity, or recovery of diseased trees to further improve the ecological realism and practical relevance of the model. Overall, the model offers valuable insights into the complex dynamics governing mango agroecosystems and provides a theoretical foundation for developing targeted conservation and management strategies.

References

[1] Vaishnavi, Kalirajan, and Ramanathan Malinidevi. "Biological and Optimal Control Model for Powdery Mildew Disease in Mango Plants and Fruits." Applications of Modelling and Simulation 9 (2025): 174-188.

[2] Kabir, Sayem, et al. "Smartphone Image Dataset for Machine Learning-Based Monitoring and Analysis of Mango Growth Stages." Data in Brief (2025): 111780.

[3] Ahmed, Sarder Iftekhar, et al. "MangoLeafBD: A comprehensive image dataset to classify diseased and healthy mango leaves." Data in Brief 47 (2023): 108941.

[4] Kaewkrajay, Chutima, et al. "Production of the biocontrol agents Meyerozyma guilliermondii and Pichia kudriavzevii using a low-cost carbon source and their ability to control mango disease in field trials." European Journal of Plant Pathology (2025): 1-15.

[5] Babar, Tauseef Khan. "King of Fruits" Under Siege: Unravelling the Implications of Climate Change on Insect Pest Dynamics." Climate Change and Mango Production. Springer, Cham, 2025. 617-674.

[6] Varma, Teena, et al. "Automatic mango leaf disease detection using different transfer learning models." Multimedia Tools and Applications 84.11 (2025): 9185-9218.

[7] Rubab, Naima, Muhammad Shan, and Aamir Hussain. "IoT-Based System for Prediction of Fungal Disease Attack on Mango Leaves." Journal of Computing & Biomedical Informatics 8.02 (2025).

[8] Mondal, Ritwika, et al. "Dynamical study on volatiles signaling in plant disease and pest-natural enemy interaction." Modeling Earth Systems and Environment 11.1 (2025): 57.

[9] Mondal, Ritwika, Dipak Kesh, and Debasis Mukherjee. "Influence of competition in modelling dynamics of plant defense with induced volatile." Modeling Earth Systems and Environment 4.3 (2018): 1197-1211.

[10] Liu, Ying Hu, et al. "Modelling tritrophic interactions mediated by induced defence volatiles." Ecological modelling 220.23 (2009): 3241-3247.

[11] Mondal, Ashok, A. K. Pal, and G. P. Samanta. "Analysis of a delayed eco-epidemiological pest–plant model with infected pest." Biophysical Reviews and Letters 14.03 (2019): 141-170.

[12] Anderson, Roy M., and Robert M. May. "Infectious diseases and population cycles of forest insects." Science 210.4470 (1980): 658-661.

[13] Anderson, Roy M., and Robert M. May. "Directly transmitted infections diseases: control by vaccination." Science 215.4536 (1982): 1053-1060.